

Simulation of Grover's quantum search algorithm in a Ising nuclear spin chain quantum computer with first and second nearest neighbour couplings

G V López, T Gorin and L Lara

Departamento de Física, Universidad de Guadalajara
Blvd. Marcelino García Barragan y Calzada Olímpica
4480 Guadalajara, Jalisco, México

E-mail: gorin@pks.mpg.de

Abstract. We implement Grover's quantum search algorithm on a nuclear spin chain quantum computer, taking into Ising type interactions between nearest and second nearest neighbours into account. The performance of the realisation of the algorithm is studied by numerical simulations with four spins. We determine the temporal behaviour of the fidelity during the algorithm, and we compute the final fidelity as a function of the Rabi frequency. For the latter, we obtained pronounced maxima at frequencies which fulfil the condition of the $2\pi k$ -method with respect to the second nearest neighbour interactions.

PACS numbers: 03.67.-a, 03.67.Lx

1. Introduction

The Ising-spin chain quantum computer is a simple theoretical model system, which has many of the relevant features of a physical realisation of a quantum computer. The bare model is defined in terms of a time-independent Hamiltonian H_0 , describing a system of spins in a strong magnetic field and coupled by the Ising-interaction. Additional time-dependent perturbations (*e.g.* radio-frequency pulses, which may be switched on and off at will) are used to implement certain elementary quantum gates, from which any unitary quantum algorithm can be constructed (universal quantum gates).

Originally, this model has been proposed in [1, 2, 3, 4], and a large number of theoretical studies has been devoted to it (to mention a few important works: [5, 6, 7]). As a physical realisation, one may think of nuclear spins embedded in a solid state system in an external strongly inhomogeneous magnetic field. Ultracold atoms in optical lattices may provide a possibly less demanding alternative [8].

In the present work, we assume an Ising-interaction between nearest and next-nearest (second) neighbours [9, 10]. In this case, the bare Hamiltonian becomes

$$\frac{1}{\hbar} H_0 = - \sum_{k=1}^n w_k I_k^z - 2J \sum_{k=1}^{n-1} I_k^z I_{k+1}^z - 2J' \sum_{k=1}^{n-2} I_k^z I_{k+2}^z, \quad (1)$$

where w_k is the Larmor frequency of spin k . Since the dipole interactions may be induced by electron clouds around the nuclear spins, it is realistic to consider J and J' as independent parameters. The Hamiltonian H_0 is diagonal in the so called computational basis, which consists of products of single spin (qubit) eigenstates of I_k^z , which are denoted by $|0_k\rangle$ and $|1_k\rangle$ respectively:

$$I_k^z |\alpha_k\rangle = \frac{(-1)^{\alpha_k}}{2} |\alpha_k\rangle. \quad (2)$$

We denote the 2^n eigenstates of H_0 by $\{|\alpha_{n-1}, \dots, \alpha_0\rangle\}$ with $\alpha_k = 0, 1$ for $k = 0, \dots, n-1$.

In order to implement the desired quantum gates, we use monochromatic electromagnetic radio-frequency pulses (RF-pulses) described by the term $W(t)$,

$$H = H_0 + W(t), \quad W(t) = \frac{\hbar\Omega}{2} \sum_{k=0}^{n-1} (e^{i(wt+\varphi)} I_k^+ + e^{-i(wt+\varphi)} I_k^-), \quad (3)$$

where the frequency w , the phase offset φ and the Rabi frequency Ω are free parameters (Ω/γ is the amplitude of the electromagnetic field and γ is the gyromagnetic ratio for the spins). $I_k^+ = (I_k^-)^\dagger = |0_k\rangle\langle 1_k|$ is the raising operator of qubit k . The desired quantum gates (and the whole quantum algorithm) are realised within the interaction picture. We apply the above defined RF-pulses with a rectangular envelope, choosing the frequency w in resonance with an appropriate transition in H_0 . The resulting unitary evolution is denoted by

$$R_k^{\mu\nu}(\varphi, \vartheta), \quad w = w_k + \mu J + \nu J', \quad (4)$$

where μ and ν are integers. The angle φ gives the phase offset of the RF-pulse, whereas $\vartheta = \Omega\tau$ determines the duration τ of the pulse. The RF-pulses are selected in such a way that they yield the desired quantum gates exactly, if all off-resonant transitions are neglected (resonant approximation). For the “real” evolution will be obtained from numerical simulations, where all transitions are taken into account. The deviation from the “ideal” evolution is quantified by fidelity [11], the absolute value squared of the wave-function overlap for both evolutions. In order to minimise the decay of fidelity, We apply the $2\pi k$ -method to suppress those transitions which are nearest to resonance. These are of order J' , and therefore related to the second neighbour interaction [10].

In the present work, we study the effects of unitary errors (due to non-resonant transitions) on a quantum algorithm of intermediate length. Such an algorithm may consist of several hundreds of pulses, even though it is still far away from the regime, where a quantum computer could really demonstrate its superiority over a classical one (after all, our work relies on numerical simulations on a classical PC). It is however also far beyond pulse sequences, which only realise one or a few elementary qubit gates. Of particular interest will be the question whether we can from the fidelity decay of few gate operations extrapolate to the fidelity decay of the whole quantum algorithm.

As an example we consider Grover's search algorithm [12, 13] which has also been implemented experimentally [14, 15, 16]. We will implement this algorithm on a spin chain of length four, where one of the spins will serve as the “ancilla” qubit. The basic elements of this algorithm are single-qubit Hadamard gates. Due to the Ising interactions, these gates are quite expensive in the Ising-spin chain quantum computer as we will see below. The big majority of the pulses are used to implement these gates. The other gates are n -qubit phase-gates, where n is the number of bits of the search space (in our case $n = 3$).

In the following section (section 2), we will discuss Grover's search algorithm as such, and its implementation in the Ising-spin chain quantum computer. In section 3, we show numerical simulations of the search algorithm, discuss the fidelity decay during the execution of the algorithm, and study this fidelity as a function of Rabi frequency. Conclusions are provided in section 4.

2. Realisation of Grover's search algorithm

In its most basic form [17], Grover's quantum search algorithm requires n qubits to prepare the “enquiry” states (in the data register) subsequently presented to the “oracle”, and a single additional qubit (the “ancilla” qubit) required by the oracle to communicate its answer. Starting from the ground state of the system, $|0_{n-1}, \dots, 0_0\rangle$, the algorithm itself consists of an initial step, where the complete superposition of all basis states is created by applying Hadamard gates to all qubits of the data register. Let us denote a single Hadamard gate applied to qubit j by H_j and the sequence of Hadamard gates to create the superposition state in m qubits by $H^{\otimes m}$. The creation of the superposition state is followed by a Grover operator, which may be repeated several

times, until the data register contains the desired target state with sufficiently high probability.

The Grover operator is again composed of Hadamard gates and conditional phase reflections:

$$G = O(\alpha) H^{\otimes m} S_0 H^{\otimes m} , \quad (5)$$

where α may be any number representable in the data register. The unitary oracle $O(\alpha)$, leaves all basis states untouched, except for the state $|\alpha\rangle$, to which it applies a sign change (phase reflection). The other unitary operator S_0 , in turn, changes the sign of all basis states but leaves the state $|0\rangle$ untouched. While the Hadamard gates are single qubit gates, $O(\alpha)$ and S_0 are true n -qubit gates.

In this work we implement the Grover algorithm in a quantum register of four qubits: $\{i_3, i_2, i_1, i_0\}$. For numerical simulations, it is convenient to use the qubits $k = 0, 2, 3$ as data register, and the qubit $k = 1$ as the ancilla qubit. In this way, the ancilla qubit is coupled directly (by first or second neighbour couplings) to all qubits in the data register. In what follows, we discuss the implementation of the Hadamard gates, the conditional phase reflection S_0 and the oracle, in separate subsections.

2.1. Hadamard gates

The Hadamard gate is a single qubit gate. In the Hilbert space of that qubit the gate acts as a unitary matrix:

$$H = \frac{1}{\sqrt{2}} \begin{pmatrix} 1 & 1 \\ 1 & -1 \end{pmatrix} . \quad (6)$$

It can be decomposed into elementary qubit rotations as follows:

$$H = R_y(\pi) R_y(\pi/2) R_x(\pi) , \quad (7)$$

where $R_x(\vartheta) = R(\pi, \vartheta)$, $R_y(\vartheta) = R(\pi/2, \vartheta)$ and

$$R(\varphi, \vartheta) = \begin{pmatrix} \cos(\vartheta/2) & i e^{i\varphi} \sin(\vartheta/2) \\ i e^{-i\varphi} \sin(\vartheta/2) & \cos(\vartheta/2) \end{pmatrix} . \quad (8)$$

The single qubit rotations of the form (8) may be obtained by applying appropriate electromagnetic pulses as defined in (3) and (4) to the Ising spin chain. In the presence of neighbouring qubits, one has to repeat that pulse sequence for all possible configurations of the neighbouring qubits, in order to obtain the true single qubit gate, independent of the state of the neighbouring qubits. Denoting the Hadamard gate applied to qubit i as H_i , we obtain specifically:

$$H_0 = \prod_{\mu=-1,1} \prod_{\nu=-1,1} R_0^{\mu\nu}(\pi/2, \pi) R_0^{\mu\nu}(\pi/2, \pi/2) R_0^{\mu\nu}(\pi, \pi) \quad (9)$$

$$H_2 = \prod_{\mu=-2,0,2} \prod_{\nu=-1,1} R_2^{\mu\nu}(\pi/2, \pi) R_2^{\mu\nu}(\pi/2, \pi/2) R_2^{\mu\nu}(\pi, \pi) \quad (10)$$

$$H_3 = \prod_{\mu=-1,1} \prod_{\nu=-1,1} R_3^{\mu\nu}(\pi/2, \pi) R_3^{\mu\nu}(\pi/2, \pi/2) R_3^{\mu\nu}(\pi, \pi) , \quad (11)$$

which implements the unitary gate $H^{\otimes 3} = H_0 H_2 H_3$ on the data register.

2.2. The conditional phase inversion S_0

Formally, the gate S_0 may be described by

$$S_0 |\alpha\rangle = (-1 + 2\delta_{\alpha,0}) |\alpha\rangle . \quad (12)$$

The (unconditional) phase inversion of the state of a single qubit may be obtained by applying the pulse $R(0, 2\pi)$ to it. In the present case, we obtain S_0 by applying $R(0, 2\pi)$ to the qubit $i = 1$ repeatedly – covering all possible configurations of its neighbouring qubits except for that case, where the data-qubits form the state $|0\rangle$. This leads to the pulse sequence

$$S_0 = R_1^{2,-1}(0, 2\pi) R_1^{0,1}(0, 2\pi) R_1^{0,-1}(0, 2\pi) R_1^{-2,-1}(0, 2\pi) R_1^{-2,1}(0, 2\pi) . \quad (13)$$

2.3. The oracle

The oracle is a unitary gate, which changes the sign of the state of the data register, depending on its contents. In the search algorithm, it is thought that any number $|\alpha\rangle$ representable in the data register serves as an index to given items in a data base. The search consists in finding the index of that item which has a certain unique property (*e.g.* the telephone number of a certain person with a certain address). In the present case, we will request that the index itself be a certain number out of the set $\{0, 5, 8, 13\}$ (decimal notation). In those cases, the oracle may be implemented by a single 2π -pulses:

$$O(0) = R_1^{2,1}(0, 2\pi) \quad (14)$$

$$O(8) = R_1^{2,-1}(0, 2\pi) \quad (15)$$

$$O(5) = R_1^{-2,1}(0, 2\pi) \quad (16)$$

$$O(13) = R_1^{-2,-1}(0, 2\pi) . \quad (17)$$

The other numbers representable in the data register are $\{1, 4, 9, 12\}$, but a oracle selecting those states would require many more qubits.

3. Numerical simulations

Our simulations normally start with the ground state, $|0000\rangle$. Then, we generate the total superposition state in the data register and perform two Grover steps. This is sufficient to obtain the desired target state with very high probability (above 95%). With the pulse sequences given in section 2, one needs 42 pulses for the initial superposition state and 90 pulses for each Grover operator step.

Unfortunately, the pulse sequence described in section 2 is not optimal in terms of accuracy. The direct implementation of the Hadamard gates according to the scheme described there, leads to prohibitively large errors. Luckily, these errors can be reduced efficiently, by recombining the pulses in the sequence for one Hadamard gate into shorter sequences implementing several single qubit gates. This can be done due to

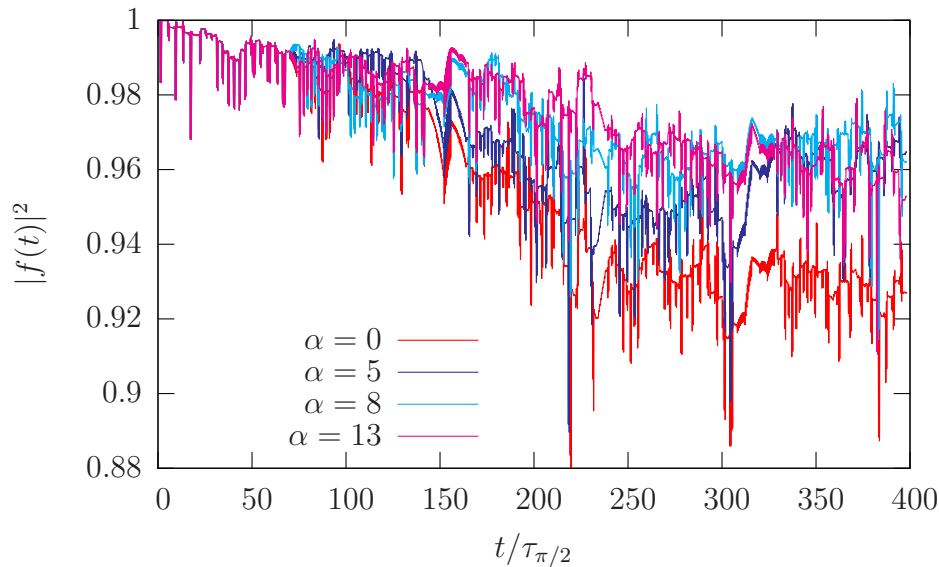


Figure 1. The absolute value squared of the fidelity during the Grover algorithm with two Grover operator steps. Time is measured in units of the duration of a single $\pi/2$ -pulse. The algorithm is simulated for different target states $|\alpha\rangle$ (see legend). The Rabi frequency is $\Omega = 0.1008$, which suppresses non-resonant transitions as far as possible.

the commutativity of the operators appearing in (9). Thus, for *e.g.* the Hadamard gate H_0 , we obtain the following pulse sequence

$$H_0 = \left\{ \prod_{\mu,\nu=-1,1} R_0^{\mu\nu}(\pi/2, \pi) \right\} \left\{ \prod_{\mu,\nu=-1,1} R_0^{\mu\nu}(\pi/2, \pi/2) \right\} \left\{ \prod_{\mu,\nu=-1,1} R_0^{\mu\nu}(\pi, \pi) \right\}, \quad (18)$$

with much smaller errors. We use similar rearrangements for H_2 and H_3 .

The overall error can be further decreased by rearranging the outer sequences of π -pulses in a similar manner into sequences of single qubit $\pi/2$ -pulses. These measures drastically increase the number of pulses for the implementation of the algorithm. Now, we need 20 pulses for the H_0 and the H_3 gate and 30 pulses for the H_2 gate. In total this gives 70 pulses for the $H^{\otimes 3}$ gate and 146 pulses for each Grover operator step. Note however that the amount of time to implement those gates is the same as before.

In this section, we are mainly concerned with unitary errors due to non-resonant transitions, and due to phase-errors which are not suppressed by the $2\pi k$ -method. Thus, we will study in some detail the behaviour of fidelity during the algorithm. The fidelity [11], $f(t)$, is the overlap between the state evolving under the ideal evolution (where only resonant transitions are taken into account) and the state evolving under the true evolution governed by the Hamiltonian in (3). The fidelity (or fidelity amplitude) is a complex quantity. Thus, we will normally study its absolute value squared, $|f(t)|^2$.

Figure 1 shows $|f(t)|^2$ during the whole search algorithm for four different target states, selected by different oracle pulses: red curve ($\alpha = 0$), blue curve ($\alpha = 5$), light blue curve ($\alpha = 8$), and pink curve ($\alpha = 13$). In these simulations, we set the Rabi frequency to $\Omega = 0.1008$, which corresponds to the $2\pi k$ -method with $k = 4$. Since k is even, non-resonant transitions are suppressed during π -pulses, as well as $\pi/2$ -pulses.

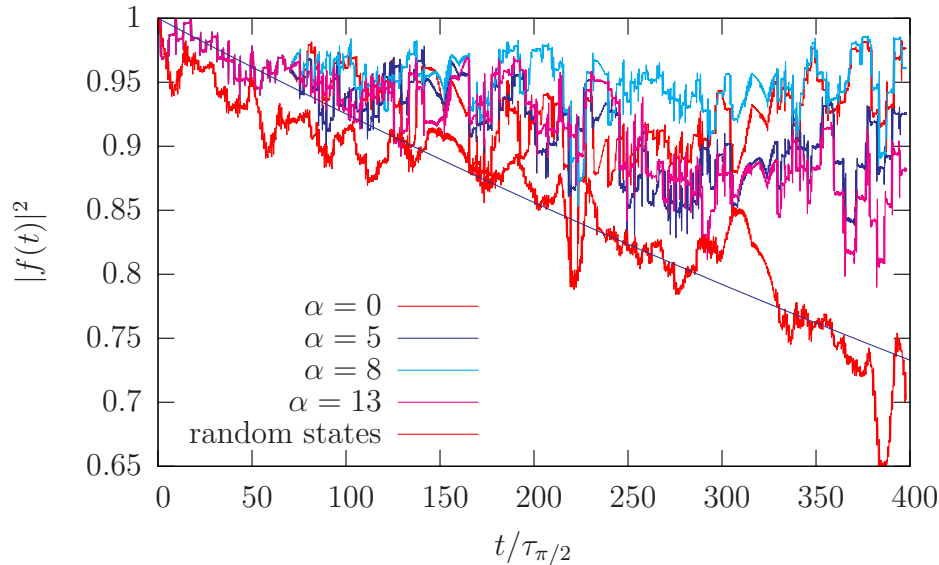


Figure 2. The absolute value squared of the fidelity during the Grover algorithm with two Grover operator steps. Time is measured in units of the duration of a single $\pi/2$ -pulse. The algorithm is simulated for different target states $|\alpha\rangle$ (see legend). The Rabi frequency is $\Omega = 0.135$, which yields similarly high fidelities as in figure 1. The smooth blue line shows an exponential, fitted to the initial decay ($t/\tau_{\pi/2} < 70$). The fastest decay, roughly following the exponential is obtained for random initial states (lowest red curve).

Figure 2 shows $|f(t)|^2$ for the same Grover algorithm, but for the Rabi frequency, $\Omega = 0.135$, which corresponds to the $2\pi k$ -method with $k = 3$. Since k is odd in this case, one would expect that non-resonant transitions are suppressed during π -pulses, but not during $\pi/2$ -pulses. Still, we find similarly high fidelities as in the previous case. This surprising result is discussed in more detail, below. In this figure, the fidelity along the full algorithm does not follow the initial trend of relatively fast decay. To obtain that initial trend, we fitted an exponential to the initial preparation step (the first 70 $\pi/2$ -pulses).

This non-generic behaviour is interesting, because it shows that it is not sufficient to characterise the performance of individual quantum gates by their average fidelity-loss rates. With no other information than such loss rates, one would greatly underestimate the overall fidelity of the algorithm. A convenient way to obtain average loss rates, is to use random initial states. The lower red curve shows $|f(t)|^2$ averaged over 100 different initial states chosen at random from the invariant (under unitary transformations) ensemble of normalised states. The curve still shows large fluctuations which should disappear in the limit of a larger sample size. However, the general trend of a global exponential decay is clearly observable. It also agrees quite nicely with the exponential fit (smooth blue curve).

In figure 3 the Rabi frequency is chosen to allow non-resonant transitions, $\Omega = 0.2550$. By consequence, we find a much faster decay of the fidelity. In distinction to

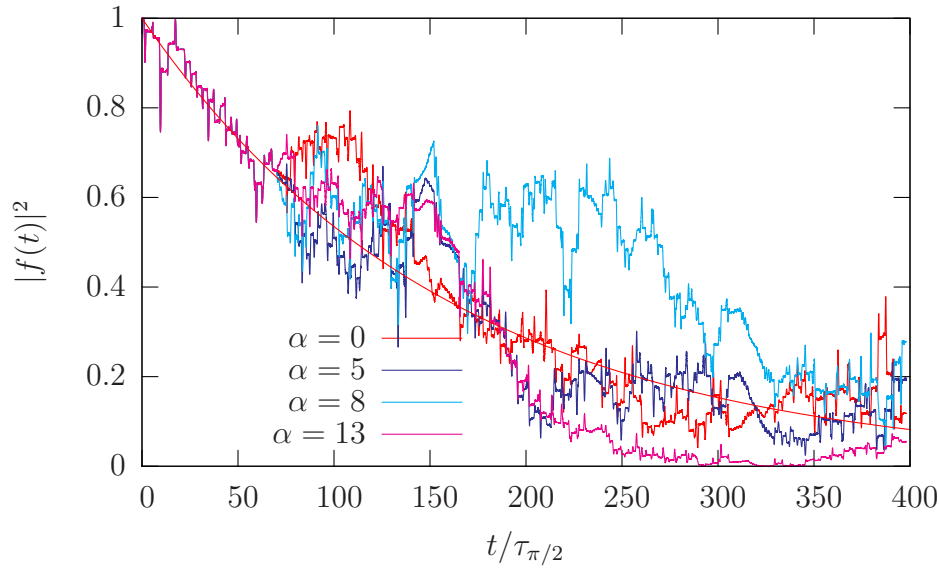


Figure 3. The fidelity (its absolute value squared) during the Grover algorithm with two Grover operator steps. Time is measured in units of the duration of a $\pi/2$ -pulse. The algorithm is simulated for different target states $|\alpha\rangle$ (see legend).

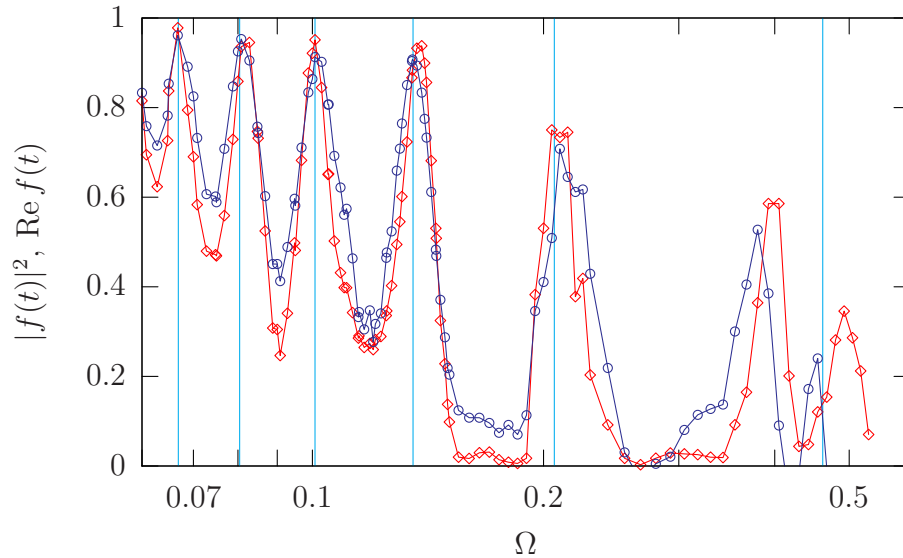


Figure 4. The fidelity (blue line) as well as its absolute value squared (red line) of the whole Grover algorithm as a function of the Rabi frequency, Ω . The algorithm is simulated for the target state $|\alpha\rangle$, $\alpha = 13$.

the previous figures, the fidelity now follows much closer an exponential decay, although there are still very large fluctuations between the different cases (different oracles).

In figure. 4 we plot the real part of the fidelity (blue line) as well as its absolute value squared (red line) for the whole algorithm with two Grover operator steps as a function of the Rabi frequency, Ω . We chose the oracle $O(13)$, which selects the target state $|\alpha\rangle$ with $\alpha = 13$. One can clearly see pronounced peaks of maximal fidelity, where

the $2\pi k$ -method is at work. The Rabi frequencies obtained from the condition of the $2\pi k$ -method are indicated by vertical lines, where k increases from $k = 1$ near $\Omega \approx 0.45$ up to $k = 6$ near $\Omega \approx 0.067$.

For integer k , the $2\pi k$ -method suppresses non-resonant transitions only for π -pulses. In order to suppress non-resonant transitions also for $\pi/2$ -pulses, k must be even. Since the present algorithm consists mainly of $\pi/2$ -pulses, we should expect rather small fidelities at Rabi frequencies which correspond to odd values for k . Nevertheless, even for odd values of k , we find pronounced maxima of maximal fidelity. They are almost as high as the maxima corresponding to even k 's. Somehow, it happens that non-resonant transitions which occur during one $\pi/2$ -pulse are undone during a second $\pi/2$ -pulse. While this might not be so surprising in the case of the π -pulses which have been split deliberately into $\pi/2$ -pulses, it is more surprising in the case of $R_y(\pi/2)$ which also forms a part of the Hadamard gate [see equation (7)], and which is implemented with "true" $\pi/2$ -pulses.

4. Conclusion

We implemented Grover's quantum search algorithm on a Ising spin chain of length four, taking into account first and second neighbour couplings. The coupling strength of second neighbours is much weaker than that of first neighbours, which means that the dominant source for errors are near resonant transitions, where the detuning is of the order of J' . In other words, the second neighbour couplings are the dominant source for errors in our setup. The accumulated error in the course of the quantum algorithm are quantified by the fidelity. We investigated its temporal behaviour as well as its final value, at the end of the algorithm, as a function of the Rabi frequency.

We found that by properly rearranging the RF-pulses, the errors in the implementation of the Hadamard gates are greatly reduced. By properly choosing the Rabi frequency we obtained fidelities beyond 90%, for the whole algorithm with two Grover steps. This corresponds to an average loss of fidelity of the order of 4×10^{-4} (per π -pulse) and 6×10^{-3} (per Hadamard gate), numbers which are compatible with recent requirements for fault tolerant quantum computation [18]. However, we also found that the loss of fidelity in different subsections of the algorithm varies considerably (sometimes even in sign), which means that it is in general not possible to estimate the fidelity of the whole algorithm, knowing the fidelities of its parts.

In the present work, we implemented the $2\pi k$ -method to suppress non-resonant transitions. Since the big majority of the RF-pulses used are $\pi/2$ -pulses, we would have expected high fidelities at Rabi frequencies corresponding to even k , but rather low fidelities at Rabi frequencies corresponding to odd k . Surprisingly, we found similarly pronounced maxima of the fidelity at Rabi frequencies corresponding to even and odd values for k .

Preliminary studies using fluctuating Larmor frequencies (simulating tiny variations of the external magnetic field) indicate that these findings are not sensitive to external

noise. A more detailed study of the effect of noise will be the subject of future investigations.

References

- [1] Lloyd S 1993 *Science* **261** 1269
- [2] Berman G P, Doolen G D , Holm D D and Tsifrinovich V I 1994 *Phys. Lett. A* **193** 444
- [3] Lloyd S 1995 *Sci. Am.* **273** 140
- [4] Bennet C H 1995 *Phys. Today* **48** 24
- [5] Berman G P, Doolen D D, López G V and Tsifrinovich V I 2000 *Phys. Rev. A* **61** 062305
- [6] Berman G P, Borgonovi F, Izrailev F M and Tsifrinovich V I 2001 *Phys. Lett. A* **291** 232
- [7] Berman G P, Kamenev D I, Doolen D D, López G V and Tsifrinovich V I 2002 *Contemp. Math.* **305** 13
- [8] García-Ripoll J J and Cirac J I 2003 *New J. Phys.* **5** 76
- [9] López G V and Lorena L 2005 *J. Phys. B: At. Mol. Opt. Phys.* **38** 3897
- [10] López G V, Gorin T and Lara L 2007 *E-print* arXiv:0705.3688v1
- [11] Gorin T, Prosen T, Seligman T H and Žnidarič M 2006 *Phys. Rep.* **435** 33
- [12] Grover L K 1997 *Phys. Rev. Lett.* **79** 325
- [13] Grover L K 1998 *Phys. Rev. Lett.* **80** 4329
- [14] Yang W L, Chen C Y and Feng M 2007 *E-print* arXiv:0707.0334v1
- [15] Feng M 2001 *Phys. Rev. A* **63** 052308
- [16] Jones J A, Mosca M and Hansen R H 1998 *Nature* **393** 3408
- [17] Nielsen M A and Chuang I L 2000 *Quantum Computation and Quantum Information* (Cambridge, Cambridge University Press)
- [18] Knill E 2004 *E-print* quant-ph/0410199